20th International Conference
"Research and Development in Mechanical Industry"
RaDMI-2020
17-20 September 2020, Sokobanja (Serbia)

Plenary and Invitation Paper

Temporary Leaning of the Gas Oil Storage Tank Structure During Bottom Sanation

Srđan M. Bošnjak[1], Nebojša B. Gnjatović[2], Aleksandar Z. Stefanović[3], Ivan LJ. Milenović[4]
[1,2,3,4] University of Belgrade-Faculty of Mechanical Engineering, Belgrade, SERBIA
[1]E-mail: sbosnjak@mas.bg.ac.rs; [2]E-mail: ngnjatovic@mas.bg.ac.rs
[3]E-mail: astefanovic@mas.bg.ac.rs; [4]E-mail: imilenovic@mas.bg.ac.rs

Abstract: *The design concept of temporary leaning of the gas oil storage tank bearing structure used during substitution of the worn out section of the bottom plates in the zone of the central column support is presented in the paper. On the basis of comparative analysis of the results obtained using finite element structural calculations of the designed state and the state of the central column leaning on the temporary supports, it was determined that by the implementation of the temporary support, the stress-strain state of the bearing structure, which corresponds to the designed stress-strain state of the construction, is obtained. Besides, the strength proof of the structure of temporary support including its welded joint to the central column is also presented in the paper.*
Keywords: *gas oil storage tank, carrying structure, temporary leaning, finite element analyses, welded joint proof of bearing capacity.*

1. Introduction

Reconstruction and redesign of structures of different purposes, besides the development of realization technology, also require a calculation of their stress-strain states in the conditions of leaning substantially differing from the designed ones [1-7].
A tank with the volume of 57700 m^3 (diameter: 63.3 m; height: 18.36 m) is used for the storage of gas oil in Tripoli harbor in Libya. After perennial exploitation the section of the bottom plates in the zone of central column leaning were damaged. In order to enable the unobstructed access and realization of the substitution technology of damaged bottom plates, the cutting and removal of the central column bottom segment was necessary. This procedure leads to the change of the leaning scheme of the tank bearing structure and requires a conduction of the comparative analysis of its stress-strain state, as well as the analysis of the stress state of the newly designed central column temporary support after the removal of the column bottom segment. The temporary support of the central column consists of two identical portal frames, Fig. 1, produced using box cross section girders made of two standard UPN 300 beams (steel quality grade S235JRG2, $\sigma_{per,I}$=15.0 kN cm^2). Joints between the portal frames' structural elements, as well as joints between the temporary support and the central column are realized with welding.

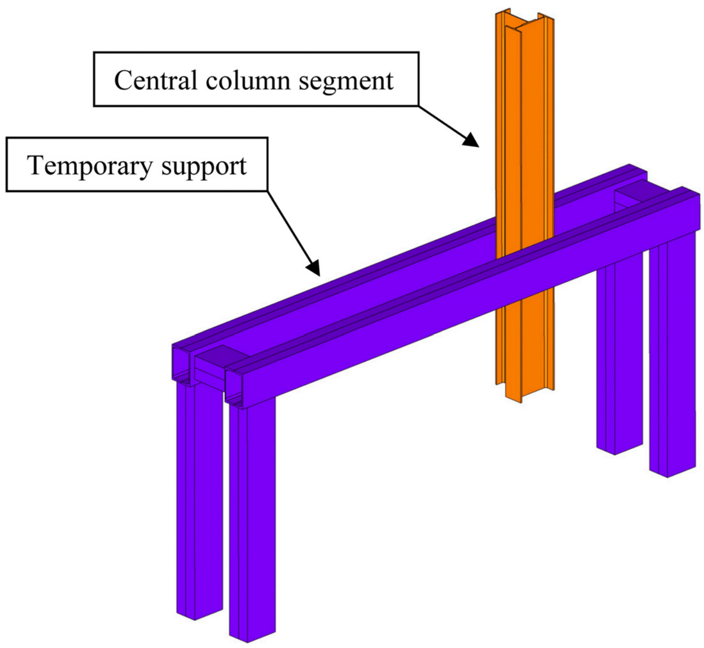

Fig. 1: Temporary support of the central column

2. Finite element model of the storage tank bearing structure

The bearing structure of the tank consists of: a central column (C1), seven columns arranged across the heptagon contour (C2), twelve columns arranged across the dodecagon contour (C3) and the bearing roof structure, which is supported by twenty columns in total (C1+7×C2+12×C3). The columns, with complex cross sections, are formed from IPE beams, Fig. 2, while the rest of the structure is realized using standard HEA, IPE, U and L beams combined with the steel girders of opened cross sections.

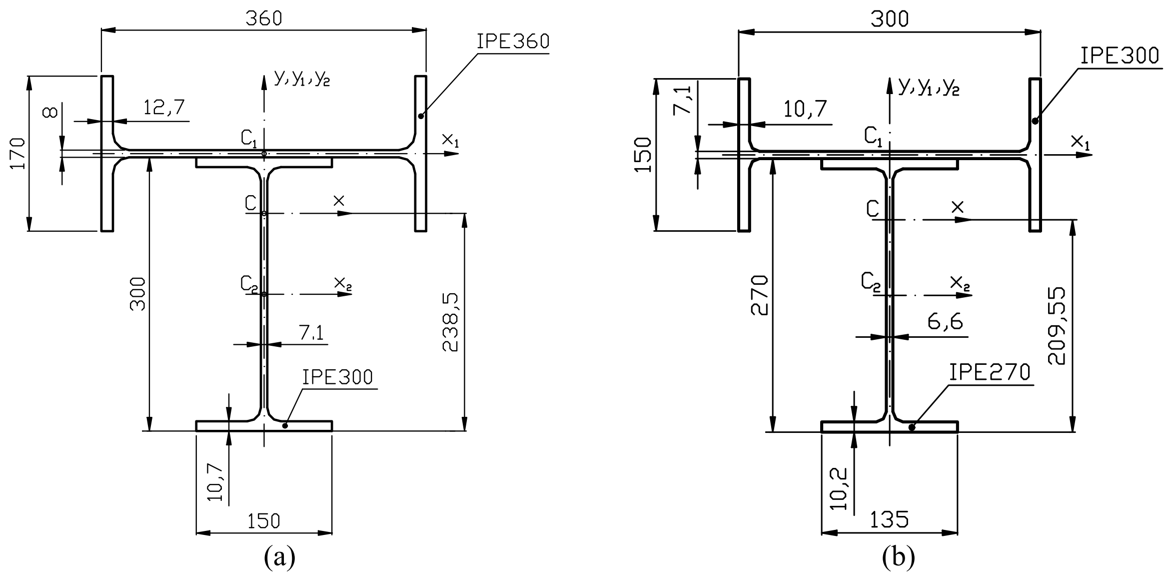

Fig. 2: Cross sections of the C1 (a) and C2, C3 (b)

The substructures of the tank are discretized using beam type finite elements, Figs. 3 an 4. Eccentricities of the system lines are simulated by introducing the so called beam type fictive elements with stiffness much higher than that of the elements of the structure. The reactions of the structure supports are determined using border elements. Finite element model of the tank bearing structure, Fig. 5, consists of 3178 nodes, 3361 beam type finite elements and 366 border elements.

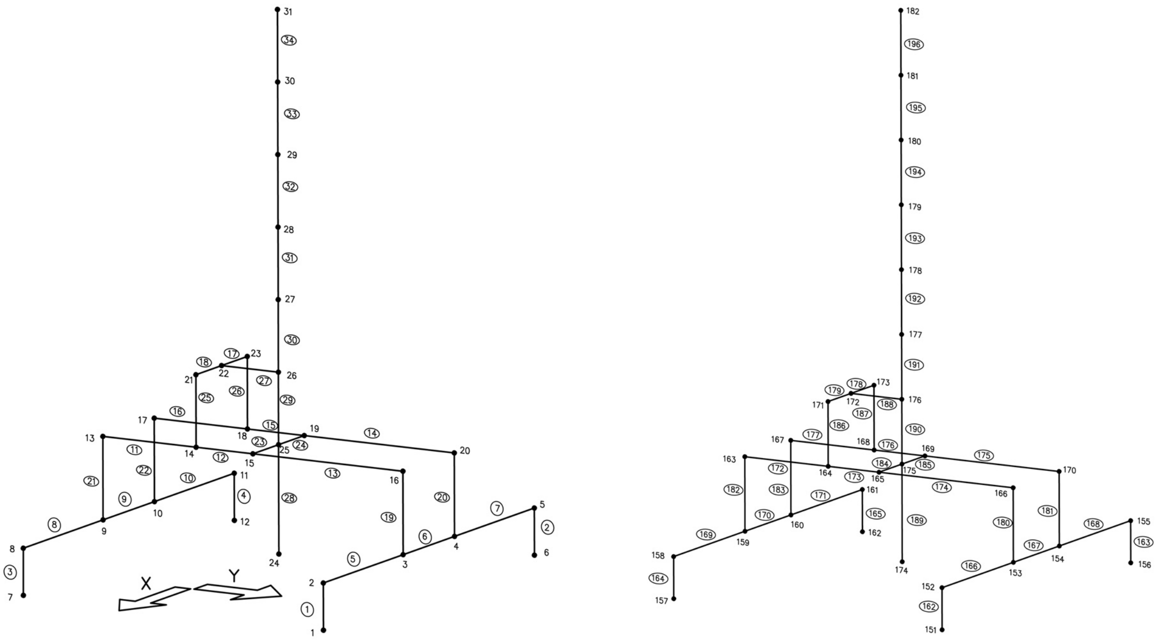

(a) (b)

Fig. 3: Finite element models of C1 (a) and C2, C3 (b)

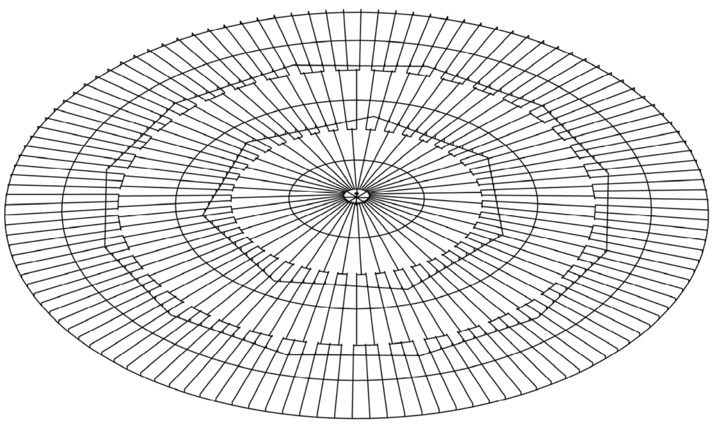

Fig. 4: Finite element model of the roof bearing structure

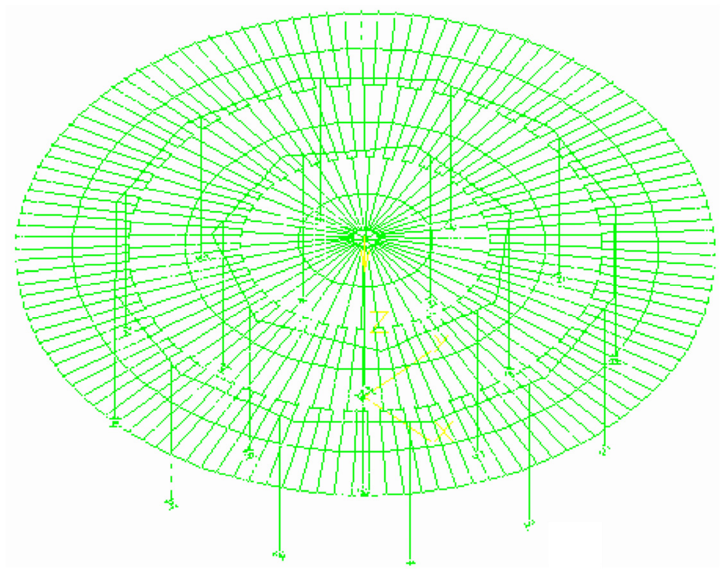

Fig. 5: Finite element model of the gas oil storage tank bearing structure

3. Calculation cases

The identification of the stress-strain state of the tank bearing structure is realized for the load case where the construction is burdened by the dead weight and the roof weight. The dead weight of the structure is treated as a continually distributed load, while the roof weight is treated as a concentrated and continually distributed load.
A finite element analysis of displacements, node loads and stresses was conducted for four referent calculation cases (CCs):

- designed state of the tank structure (CC 1),
- the state after removal of the central column's bottom segment (CC 2),
- the state after implementation of the central column's temporary support (CC 3),
- designed state of the tank structure when the vertical displacement of the central column tip (node 31), which represents the difference of the mentioned displacement obtained comparing the results of CCs 3 and 1, is implemented not taking into account the weights of the structure and roof (CC 4).

4. Stress-strain states of the tank structure and the temporary support for the referent CCs

Stress-strain states of the tank structure obtained for the analyzed CCs are presented in Figs. 6-9. On the basis of stress-strain state of the tank structure obtained for CC 2, Fig. 7, it is conclusive that the elimination of C1 from the leaning system leads to the appearance of unacceptably high stress and displacement values, drawing the conclusion that the implementation of the temporary support of C1 is mandatory. On the other hand, based on the comparative analysis of the stress-strain state of the tank bearing structure obtained for the CCs 1 and 3, it is conclusive that the implementation of the temporary support preserves the distribution of loads and stresses which corresponding to the design state, while the difference between vertical displacements of the C1 tip (node 31) in the said calculation cases equals to $\Delta z_{31}=z_{31,CC3}-z_{31,CC1}=-1.9-(-1.2)=-0.7$ mm. The highest stress response of the structure to the vertical displacement of the node 31 calculated in this manner equals to 0.2 kN/cm^2, Fig. 9, representing a negligibly small stress increment. Taking also into account the fact that the maximum stress value which appears on the structure of the temporary support is 3.7 kN/cm^2 (CC 3), it is conclusive that stiffness and strength of the newly designed temporary support of the C1 provide safe leaning of the tank bearing structure during replacement of the section of bottom plates beneath the C1, without the appearance of permanent deformations which would jeopardize the designed geometry of the structure.

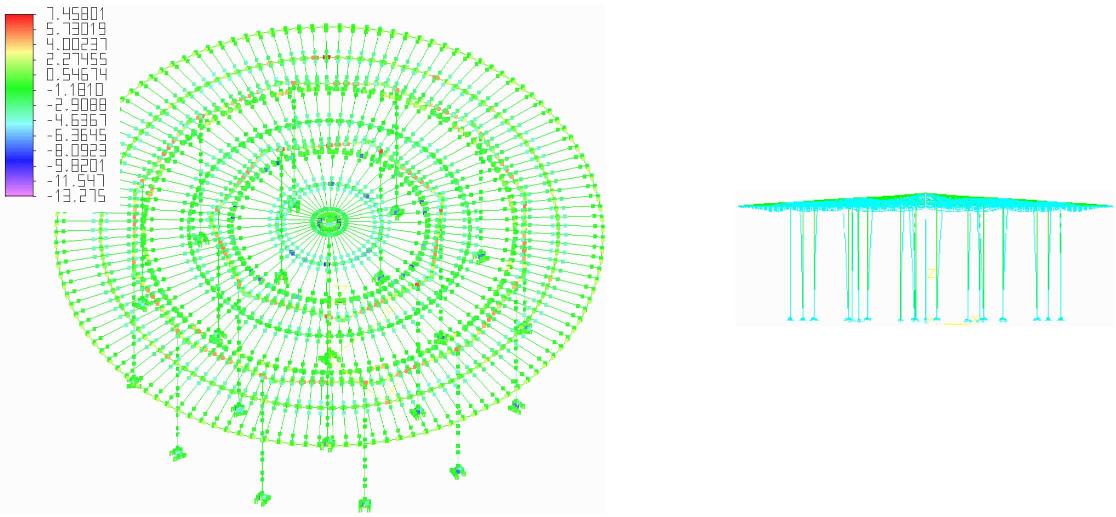

(a) (b)

Fig. 6: Stress (a)-strain (b) state of the structure in CC 1:
maximum stress value 7.5 kN/cm^2; vertical displacement of the tip of C1: $z_{31,CC1}=-1.2$ mm

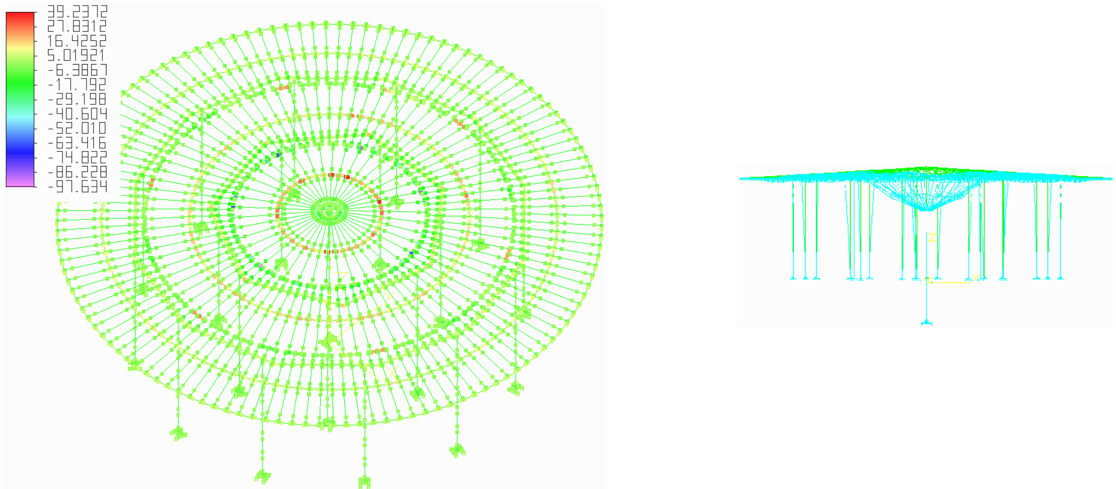

(a) (b)

Fig. 7: Stress (a)-strain (b) state of the structure in CC 2:
maximum stress value 39.2 kN/cm^2; vertical displacement of the tip of C1: $z_{31,CC2}$=–151.5 mm

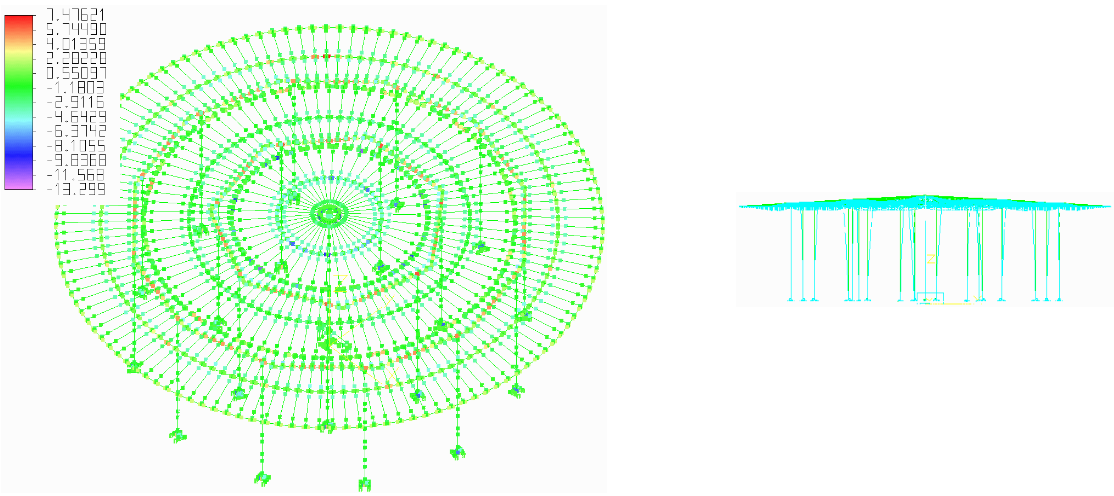

(a) (b)

Fig. 8: Stress (a)-strain (b) state of the structure in CC 3:
maximum stress value 7.5 kN/cm^2; vertical displacement of the tip of C1: $z_{31,CC3}$=–1.9 mm

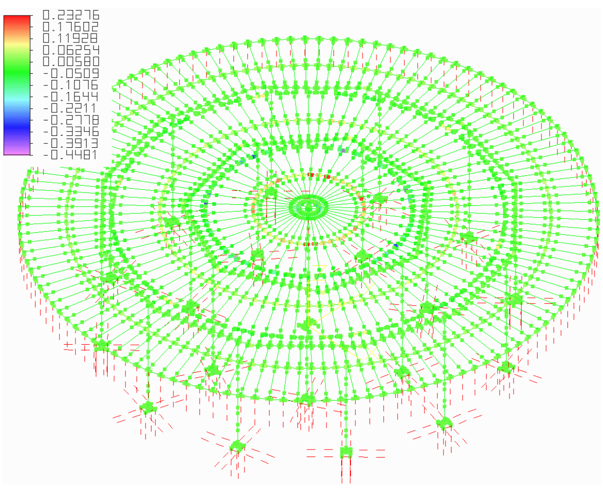

Fig. 9: Stress state of the structure in CC 4: maximum nominal stress value 0.2 kN/cm^2

5. Proof of welded joints bearing capacity

5.1. Welded joint between the central column and the temporary support

Welded joint between the central column and the temporary support is realized using a fillet weld with the thickness of 5 mm, Figs. 10 and 11. The data on the geometry and loading, as well as calculation procedures for the welded joints "A" and "B" are presented in Tables 1-4. Permitted stress value of fillet welds used to join structural elements made of steel quality grade S235JRG2 equals to σ_{per}=13.5 kN cm^2 [8].

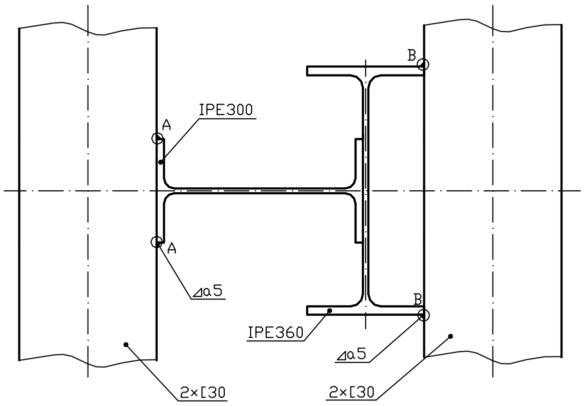

Fig. 10: Welded joint between the central column and the temporary support

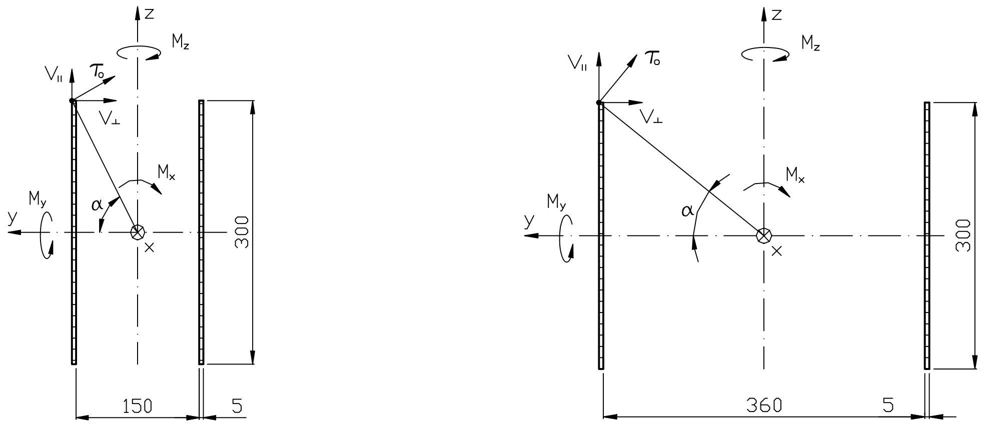

(a) (b)

Fig. 11: (a) Welded joint between the flange of IPE 300 and the horizontal girder of the temporary support (welded joint “A” in Fig. 10); (b) Welded joint between the flange of IPE 360 and the horizontal girder of the temporary support (welded joint “B” in Fig. 10)

Table 1: Geometry and loading of the welded joint “A”

Input data		
Nomenclature	Notation	Value
Geometry of the welded joint		
Thickness of the fillet welds	a	5 mm
Length of the fillet welds	l	300 mm
Distance between the centres of gravity of the fillet weld and the welded joint	d	77.5 mm
Loading of the welded joint (FEM analysis, CC 3)		
Shearing force	F_z	59.2 kN
Moment of torsion	M_x	84.0 kNcm
Bending moment about the y axis	M_y	592.0 kNcm
Bending moment about the z axis	M_z	2.05 kNcm

Table 2: Proof of welded joint "A" bearing capacity

Nomenclature	Formula	Value
Area of the fillet welds	$A = 2al$	30 cm^2
Fillet welds area moment of inertia with respect to the *y* axis	$I_y = \frac{2al^3}{12}$	2250 cm^4
Fillet welds area moment of inertia with respect to the *z* axis	$I_z = 2\left(\frac{a^3 l}{12} + ald^2\right)$	1802.5 cm^4
Fillet welds polar moment of inertia	$I_0 = I_y + I_z$	4052.5 cm^4
The distance of the most distant point of the fillet weld contour from the welded joint center of gravity	$r_{max} = \sqrt{(0.5l)^2 + (0.5d + a)^2}$	17 cm
Angle of the radius vector of the most distant point of the fillet weld contour	$\alpha = arctg \frac{l}{d + 2a}$	61°54'
Shear stres caused by the action of force F_z	$V_{ll,F_z} = \frac{F_z}{A}$	1.97 kN/cm^2
The highest value of shear stress caused by the action of the moment of torsion M_x	$\tau_{0,M_x} = \frac{M_x}{I_0} r_{max}$	0.35 kN/cm^2
Component of the shear stress $\tau_{0,Mx}$ along the fillet weld contour	$V_{ll,M_x} = \tau_{0,M_x} \cos\alpha$	0.16 kN/cm^2
Component of the shear stress $\tau_{0,Mx}$ perpendicular to the fillet weld contour	$V_{\perp,M_x} = \tau_{0,M_x} \sin\alpha$	0.31 kN/cm^2
Normal stress caused by the action of bending moment M_y	$n_{M_y} = \frac{M_y}{I_y} z_{max}$	3.95 kN/cm^2
Normal stress caused by the action of bending moment M_z	$n_{M_z} = \frac{M_z}{I_z} y_{max}$	0.01 kN/cm^2
Maximum equivalent stress in fillet weld	$\sigma_{eq} = \sqrt{\left(V_{ll,F_z} + V_{ll,M_x}\right)^2 + V_{\perp,M_x}^2 + \left(n_{M_y} + n_{M_z}\right)^2}$	4.51 kN/cm^2
Proof of welded joint bearing capacity	$\sigma_{eq} = 4.51$ kN/cm$^2 < \sigma_{per} = 13.5$ kN/cm^2	

Table 3: Geometry and loading of the welded joint "B"

Input data		
Nomenclature	Notation	Value
Geometry of the welded joint		
Thickness of the fillet welds	a	5 mm
Length of the fillet welds	l	300 mm
Distance between the centres of gravity of the fillet weld and the welded joint	d	182.5 mm
Loading of the welded joint (FEM analysis, CC 3)		
Shearing force	F_z	64.5 kN
Moment of torsion	M_x	182.3 kNcm
Bending moment about the *y* axis	M_y	645.0 kNcm
Bending moment about the *z* axis	M_z	2.1 kNcm

Table 4: Proof of welded joint "B" bearing capacity

Nomenclature	Formula	Value
Area of the fillet welds	$A = 2al$	30 cm^2
Fillet welds area moment of inertia with respect to the *y* axis	$I_y = \dfrac{2al^3}{12}$	2250 cm^4
Fillet welds area moment of inertia with respect to the *z* axis	$I_z = 2\left(\dfrac{a^3 l}{12} + ald^2\right)$	9992.5 cm^4
Fillet welds polar moment of inertia	$I_0 = I_y + I_z$	12242.5 cm^4
The distance of the most distant point of the fillet weld contour from the welded joint center of gravity	$r_{max} = \sqrt{(0.5l)^2 + (0.5d + a)^2}$	23.8 cm
Angle of the radius vector of the most distant point of the fillet weld contour	$\alpha = arctg \dfrac{l}{d + 2a}$	39°2'
Shear stres caused by the action of force F_z	$V_{ll,F_z} = \dfrac{F_z}{A}$	2.15 kN/cm^2
The highest value of shear stress caused by the action of the moment of torsion M_x	$\tau_{0,M_x} = \dfrac{M_x}{I_0} r_{max}$	0.35 kN/cm^2
Component of the shear stress $\tau_{0,Mx}$ along the fillet weld contour	$V_{ll,M_x} = \tau_{0,M_x} \cos\alpha$	0.27 kN/cm^2
Component of the shear stress $\tau_{0,Mx}$ perpendicular to the fillet weld contour	$V_{\perp,M_x} = \tau_{0,M_x} \sin\alpha$	0.22 kN/cm^2
Normal stress caused by the action of bending moment M_y	$n_{M_y} = \dfrac{M_y}{I_y} z_{max}$	4.30 kN/cm^2
Normal stress caused by the action of bending moment M_z	$n_{M_z} = \dfrac{M_z}{I_z} y_{max}$	0.01 kN/cm^2
Maximum equivalent stress in fillet weld	$\sigma_{eq} = \sqrt{\left(V_{ll,F_z} + V_{ll,M_x}\right)^2 + V_{\perp,M_x}^2 + \left(n_{M_y} + n_{M_z}\right)^2}$	4.94 kN/cm^2
Proof of welded joint bearing capacity	$\sigma_{eq} = 4.94 \text{ kN/cm}^2 < \sigma_{per} = 13.5 \text{ kN/cm}^2$	

5.2. Welded joint between the horizontal girder and the leg of the temporary support

The connection between the horizontal girder and the leg of the temporary support is realized along the entire contour of the leg cross section, Fig. 12, using the fillet weld of 5 mm thickness. Data on geometry and loading of the welded joint are provided in Table 5, while the calculation procedure is presented in Table 6.

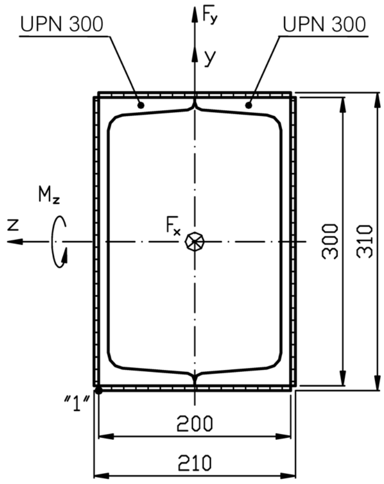

Fig. 12: Welded joint between the horizontal girder and the leg of the temporary support

Table 5: Geometry and the loading of the welded joint between the horizontal girder and the leg of the temporary support

Input data		
Nomenclature	Notation	Value
Geometry of the welded joint		
Thickness of the fillet welds	a	5 mm
The width of the leg cross section	b	200 mm
The height of the leg cross section	h	300 mm
Loading of the welded joint (FEM analysis, CC 3)		
Axial force	F_x	52.1 kN
Shearing force	F_y	182.3 kNcm
Bending moment about the *z* axis	M_z	2262.0 kNcm

Table 6: The proof of bearing capacity of the welded joint between the horizontal girder and the leg of the temporary support

Nomenclature	Formula	Value
Area of the fillet welds	$A = 2a(b+h)$	50 cm^2
Area of the fillet welds alonge the direction of *y* axis	$A_y = 2ah$	30 cm^2
Fillet welds area moment of inertia with respect to the *z* axis	$I_z = 2\left[\frac{ah^3}{12} + \frac{ba^3}{12} + \frac{ab}{2}(a+h)^2\right]$	6901.7 cm^4
Shear stres caused by the action of force F_y	$V_{ll,F_y} = \frac{F_y}{A_y}$	0.38 kN/cm^2
Normal stress caused by the action of the axial force F_x	$n_{F_x} = \frac{F_x}{A}$	1.04 kN/cm^2
Normal stress caused by the action of the bending moment M_z	$n_{M_z} = \frac{M_z}{I_z} y_{max}$	5.08 kN/cm^2
Maximum equivalent stress in the fillet weld	$\sigma_{eq} = \sqrt{V_{ll,F_y}^2 + \left(n_{F_x} + n_{M_z}\right)^2}$	6.13 kN/cm^2
Proof of welded joint bearing capacity	$\sigma_{eq} = 6.13 \text{ kN/cm}^2 < \sigma_{per} = 13.5 \text{ kN/cm}^2$	

6. Conclusion

Removal of the column's bottom segment of the bearing structure of the gas oil storage tank was the procedure which was necessary to conduct in order to enable substitution of the worn out section of the bottom plates. Results of the finite element analysis for the case of elimination of the central column from the leaning system have pointed out the appearance of unacceptably high stress states, which would inevitably lead to plastification of the storage tank bearing construction, as well as permanent distortion of its geometry. For this reason, the temporary support of the central column was designed, geometrically shaped in a manner that enables undisturbed substitution of the bottom plates of the tank. Based on the comparative analysis of the results of FEM calculations, it was determined that the stress-strain state, which corresponds to the designed stress-strain state of the tank bearing structure, is preserved by the implementation of the temporary support. Furthermore, proofs of bearing capacity for the structural elements of the temporary support and their welded joints, as well as the welded joint between the central column and the temporary support are enclosed in the paper.

Acknowledgement

This work is a contribution to the Ministry of Education, Science and Technological Development of Serbia funded project "Integrated research in the fields of macro, micro and nano mechanical engineering" (Contract number: 451-03-68/2020-14/200105).

References

[1] Petković, Z.; Bošnjak, S. & Gašić, V.: Comparative stress/deformation analysis of temporary support for reconstruction of furnace modeled with linear, shell and solid finite elements. In: *Proceedings of the 4th International Conference "Research and Development in Mechanical Industry" (RaDMI-2004),* Vol. 2; Zlatibor, Serbia and Montenegro; 31. August-04. September 2004. Kraljevo (Serbia and Montenegro): Faculty of Mechanical Engineering and Trstenik (Serbia and Montenegro): High Technical Mechanical School, 2004, pp. 729-735. ISBN-10 86-83803-17-1 and ISBN-13 978-86-83803-17-0.

[2] Bošnjak, S.; Petković, Z.; Zrnić, N.; Simić, G. & Simonović, A.: Cracks, repair and reconstruction of bucket wheel excavator slewing platform. *Engineering Failure Analysis*, Vol. 16, No. 5 (2009), pp. 1631-1642. ISSN 1350-6307. https://doi.org/10.1016/j.engfailanal.2008.11.009.

[3] Petković, Z.; Bošnjak, S. & Gašić, V.: Redesign of the tribune structure in the Belgrade Arena Hall. *Machine Design*, Vol. 3, No. 1 (2011), pp. 41-46. ISSN 1821-1259.

[4] Bošnjak, S.; Pantelić, M.; Zrnić, N.; Gnjatović, N. & Đorđević, M: Failure analysis and reconstruction design of the slewing platform mantle of the bucket wheel excavator O&K SchRs 630. *Engineering Failure Analysis*, Vol. 18, No. 2 (2011), pp. 658-669. ISSN 1350-6307. https://doi.org/10.1016/j.engfailanal.2010.09.035.

[5] Petković, Z.; Gnjatović, N.; Milenović, I.; Milojević, G. & Stefanović, A.: Design of unique below-the-hook lifting devices for specific loads. In: *Proceedings of the 14th International Conference "Research and Development in Mechanical Industry" (RaDMI-2014),* Vol. 1; Topola, Serbia; 18-21 September 2014. Vrnjačka Banja (Serbia): SaTCIP Publisher Ltd., 2014, pp.44-51. ISBN 978-3-03835-751-3.

[6] Bošnjak, S.; Savićević, S.; Gnjatović, N.; Milenović, I. & Pantelić, M.: Disaster of the bucket wheel excavator caused by extreme environmental impact: Consequences, rescue and reconstruction. *Engineering Failure Analysis*, Vol. 56 (2015), pp. 360-374. ISSN 1350-6307. https://doi.org/10.1016/j.engfailanal.2015.01.002.

[7] Petković, Z.; Gnjatović, N.; Milenović, I.; Milojević, G. & Stefanović, A.: Specific engineering challenges during the large-scale structures' mantling and dismantling procedures. In: *Proceedings of the 21st International Conference on Material Handling, Constructions and Logistics (MHCL '15)*; Vienna, Austria; 23-25 September 2015. Belgrade (Serbia): University of Belgrade-Faculty of Mechanical Engineering, 2015, pp. 235-240. ISBN 978-86-7083-863-5.

[8] Petković, Z. & Ostrić, D.: *Metal Constructions in Machine-Building:1.* Belgrade: University of Belgrade-Faculty of Mechanical Engineering, 1996. – pp. 316. ISBN 86-70803-274-7.1.